



Study of the carbon dioxide chemical fixation—activation by guanidines

Fernanda Stuani Pereira^a, Eduardo Ribeiro deAzevedo^b, Eirik F. da Silva^c, Tito José Bonagamba^b, Deuber L. da Silva Agostíni^a, Alviçler Magalhães^b, Aldo Eloizo Job^a, Eduardo R. Pérez González^{a,*}

^aDepartamento de Física, Química e Biologia, Faculdade de Ciências e Tecnologia, UNESP, C.P. 467, Presidente Prudente, 19060-080 SP, Brazil

^bInstituto de Física de São Carlos, Universidade de São Paulo, C.P. 369, São Carlos, 13560-970 SP, Brazil

^cSINTEF Materials and Chemistry, R. Birkelands vei 2B, NO-7465 Trondheim, Norway

ARTICLE INFO

Article history:

Received 22 July 2008

Accepted 1 August 2008

Available online 9 August 2008

ABSTRACT

Fixation of CO₂ is one of the most important priorities of the scientific community dedicated to reduce global warming. In this work, we propose new methods for the fixation of CO₂ using the guanidine bases tetramethylguanidine (TMG) and 1,3,4,6,7,8-hexahydro-2H-pyrimido[1,2-a]-pyrimidine (TBD). In order to understand the reactions occurring during the CO₂ fixation and release processes, we employed several experimental methods, including solution and solid-state NMR, FTIR, and coupled TGA–FTIR. Quantum mechanical NMR calculations were also carried out. Based on the results obtained, we concluded that CO₂ fixation with both TMG and TBD guanidines is a kinetically reversible process, and the corresponding fixation products have proved to be useful as transcarboxylating compounds. Afterward, CO₂ thermal releasing from this fixation product with TBD was found to be an interesting process for CO₂ capture and isolation purposes.

© 2008 Elsevier Ltd. All rights reserved.

1. Introduction

There is at present great concern surrounding anthropogenic CO₂ emissions.¹ One of the options actively being pursued to reduce CO₂ emissions is Carbon Capture and Storage technology (CCS).² A key step in many CCS technologies is reversible binding of the CO₂ molecule. Identification of new mechanisms and compounds for reversibly binding CO₂ is therefore of considerable interest. One of the goals of the present work is to explore new compounds that may bind CO₂.

While CO₂ presents an environmental issue as a greenhouse gas, it is also environmentally benign in comparison with many other chemical substrates. The development of suitable methods, at laboratory scale for the preparation of interesting CO₂ containing compounds, like organic carbonates and urethanes, by respective reaction of alcohols³ or amines⁴ with CO₂, could be an alternative to avoid the use of the highly toxic phosgene and its derivatives (e.g., chloroformates).^{5,6} The use of phosgene requires secure conditions.⁶ For this reason, industries that prepare pesticides of the carbamate class using phosgene in the process need special adjacent storage areas to avoid transportation and long-term stock.

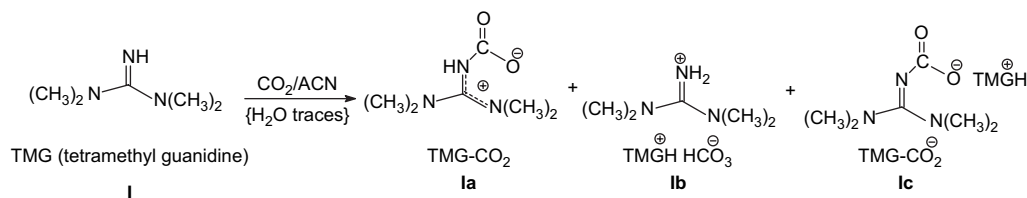
Nature of CO₂ fixation by nitrogenated bases. CO₂ transfer by transcarboxylation of amines. A new process for the formation of

a carbamic (zwitterionic) complex DBU–CO₂ from the reaction of CO₂ with 1,8-diazabicycloundecene (DBU) in fresh acetonitrile has recently been proposed.^{7a} In the same work, the transcarboxylating activity of this adduct toward some amines to yield ethyl carbamates upon O-alkylation with ethyl iodide has also been demonstrated. Subsequently, more detailed theoretical and experimental studies of the CO₂-fixation products with DBU and pentamethyldiazabicyclodecene (PMDDBD) amidines by solution NMR, thermogravimetric analyses (TGA), and X-ray diffraction methods have shown the formation of other products characterized as dimeric crystalline bicarbonates.^{7b}

More recently, the formation of carbamic intermediates by CO₂ reaction with amidines and pyridinic bases and the participation (intermediates or catalysts) of these carbamic adducts in reactions involving carbon dioxide has been also proposed.^{8,9} The formation of a zwitterionic carbamic complex by the reaction of CO₂ with DBU was investigated and this class of product was not detected.¹⁰ However, the possible formation (traces) of the carbamic product was observed. On the other hand, bicarbonates formed as CO₂-fixation products have been found to be interesting products (e.g., ionic solvents)¹¹ or useful intermediates as transcarboxylating compounds.^{7b,12}

In the present work, we describe a study of carbon dioxide fixation and release by guanidines and the nature of the guanidine–CO₂ complexes. Fixation of carbon dioxide can be a reversible process under moderate conditions (low or moderate temperature, normal pressure, etc.). At the same time, releasing CO₂ can involve a transcarboxylation process leading to several nucleophiles.⁷ For

* Corresponding author. Tel.: +55 18 3229 5355; fax: +55 18 3221 5682.
E-mail address: eperez@fct.unesp.br (E.R. Pérez González).

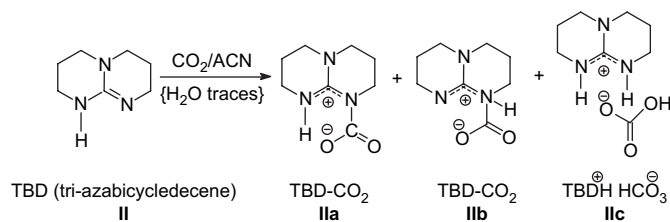


Scheme 1.

synthesis purpose, a CO_2 fixation-release occurring as a reaction process (transcarboxylation) is more interesting because it is a kinetically reversible fixation. On the other hand, for other purposes, such as industrial uses, a more thermodynamically stable fixation could be more suitable with the CO_2 being fixed and released as the unique product.

Fixation of CO_2 with the guanidine bases TMG and TBD. The structures proposed for products formed by the fixation of CO_2 with the guanidine TMG **I** are illustrated in Scheme 1. The carbamic and the bicarbonate products are represented by structures **Ia–Ic**.

It is possible to speculate that three products could be expected from the reaction of the guanidine TBD represented by the structure **II** with carbon dioxide, two tautomers presenting carbamic groups as shown in **IIa** and **IIb** and bicarbonate represented by **IIc**. All representative structures are depicted in Scheme 2.



Scheme 2.

2. Quantum mechanical calculations

All chemical species were optimized in vacuum at B3LYP/6-311++G(d,p) level of theory.¹¹ The NMR nuclear shielding was computed by using gauge-invariant atomic orbitals (GIAOs) at this level of theory. The chemical shifts were calculated with tetramethylsilane as reference. To test the sensitivity of the results to the level of theory some calculations were carried out at the MPW1PW91 level. This method has been reported to perform well in ^{13}C NMR calculations.¹³

To attempt to capture effects of the environment on the chemical shifts and reaction energies some calculations were carried out with the IEFPCM continuum solvation model.¹⁴ We carried out calculations with the acetonitrile parameters in IEFPCM. All quantum mechanical calculations were performed in Gaussian 03.¹⁵

In Table 1, we show the calculated ^{13}C NMR chemical shifts for different TMG and TBD species at B3LYP level of theory. Results with acetonitrile as solvent and at the MPW1PW91 level of theory (shown in Supplementary data) did not differ at a qualitative level from the gas phase B3LYP results.

From B3LYP level energy calculations all reactions were found to be endothermic (results shown in Supplementary data). While these results are qualitative in nature they do suggest that the CO_2 bound complexes are not stable in vacuum. This would again suggest that the species formed are to some extent stabilized by intramolecular bonding. In gas phase it was found that **IIb** was 27 kcal/mol less stable than **IIa**, suggesting that this species is unlikely to be formed in significant amounts.

Table 1

Gas phase ^{13}C NMR chemical shifts calculated at B3LYP/6-311++G(d,p) level of theory (unit is ppm)

	C1 ^a	C2–C5 ^b	$\text{CO}_2/\text{HCO}_3^-$		
TMG	173.7	41.0 (38.9, 42.5, 41.8, 40.9)			
TMGH	166.2	41.3 (39.8, 42.7, 42.7, 39.8)			
TMG– CO_2 (Ia)	168.2	40.8 (42.4, 41.5, 38.8, 40.7)	145.4		
TMG– CO_2 (Ic) ^c	152.3	41.6 (42.2, 42.6, 41.7, 40.1)	167.9		
TMGH– HCO_3^- (1) ^d (Ib)	175.1	40.9 (39.4, 40.7, 42.8, 40.5)	168.2		
TMGH– HCO_3^- (2) ^d (Ib)	173.4	40.5 (40.1, 41.6, 42.1, 38.5)	164.4		
	C4 ^e	C1 ^e	C2 ^e	C3 ^e	$\text{CO}_2/\text{HCO}_3^-$
TBD	152.9	48.9, 44.4	27.2, 28.7	51.6, 52.4	
TBDH	155.0	43.9, 43.9	24.1, 24.1	50.9, 50.9	
TBD– CO_2 (IIa)	159.1	42.9, 41.1	25.7, 25.7	53.0, 51.0	151.6
TBD– CO_2 (IIb)	153.6	49.9, 49.2	24.3, 21.4	47.8, 51.0	148.4
TBDH– HCO_3^- (IIc)	155.5	40.9, 40.9	25.9, 25.8	50.8, 50.8	168.8

^a Carbon bond to all nitrogens.

^b CH_3 groups. Average shown, followed in parenthesis by values for each atom.

^c Species not stable in gas phase, results obtained with N–C(CO_2) bond constrained to 1.6 Å.

^d Two different bicarbonate geometries were studied, geometries shown in Supplementary data.

^e Groups numbered as in Figure 3a.

3. Results and discussion

Fixation of CO_2 with TMG and TBD guanidines. The reactions were carried out under two sets of conditions, in the presence or absence of organic solvent (fresh acetonitrile). This was not difficult for TMG, but for TBD, previously melted TBD was not found to be an efficient method for CO_2 fixation. Thus, a minimal amount of acetonitrile was added to ensure a better contact of the CO_2 with the guanidine. In the case of TMG, no significant differences were observed under solvent or dry conditions. Hence, fixation of CO_2 with TMG can be proposed as a ‘green’ fixation-activation procedure with a high yield of the fixation products (90%). TBD– CO_2 products were obtained in acetonitrile with an 85% yield. Both reactions were carried out under normal pressure CO_2 (10 mL/min) and 5 mmol of guanidine was used. Reaction was carried out without any special experimental requirements. Solvent was not dried in order to achieve the CO_2 fixation by an easy and low cost. Products were characterized without any previous purification.

3.1. NMR analysis

^{13}C and ^1H NMR of the TMG– CO_2 . In the first attempt to characterize the reaction, products of the CO_2 fixation by TMG, solution ^1H and ^{13}C NMR spectra were acquired. However, the TMG– CO_2 reaction product was not completely soluble in CDCl_3 and a white powder precipitation was observed. In addition, free CO_2 was released from the solution. Despite that ^1H and ^{13}C NMR experiments were carried out in the liquid phase to characterize the soluble part of the product, resulting in the spectra shown in Figure 1a and b. These spectra can be assigned considering the TMG structure (without the CO_2 fixation) as shown in Figure 1a. Therefore, these results indicate that interaction with the solvent produced the

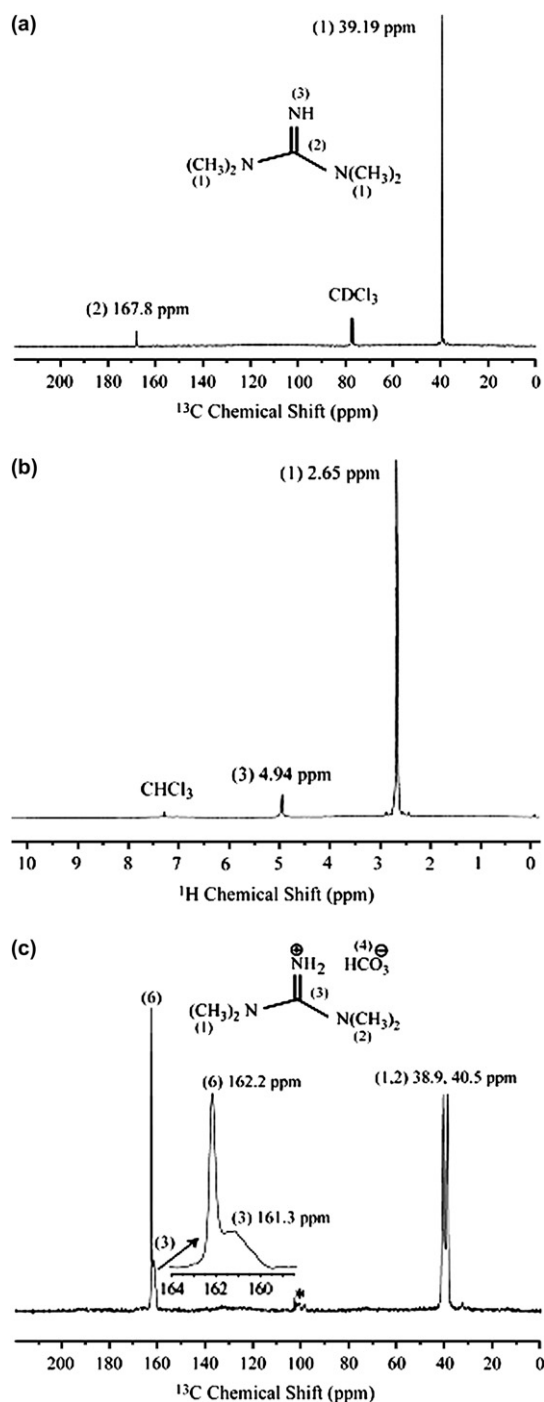


Figure 1. Solution ^{13}C (a) and ^1H (b) NMR spectra of the CDCl_3 soluble portion of the TMG- CO_2 reaction product (only TMG is detected; structure **I** in Scheme 1). Both spectra (a and b) are not quantitative because they were not performed in the fully relaxed conditions. (c) ^{13}C CP/MAS spectrum of the non- CDCl_3 soluble portion of the TMG- CO_2 reaction product (represented by **Ib** in Scheme 1). The inset shows a zoom of the 158–166 ppm region. Spinning side bands are indicated by asterisk (*) in the spectrum.

dissociation of one of the reaction products resulting in the release of CO_2 while the TMG remained dissolved in CDCl_3 . However, there was also the precipitation of another reaction product, which was characterized using solid-state ^{13}C Cross-Polarization Magic-Angle Spinning (^{13}C CP/MAS) NMR experiments (Fig. 1c). Four lines at 38.9 (1), 40.5 (2), 161.3 (3), and 162.2 ppm (4) can be observed in the spectrum shown in Figure 1c. The ^{13}C NMR lines within the 39–44 ppm region have typical chemical shift values of methyl

carbons in NCH_3 groups, while the line in the 160–163 ppm region could be either from guanidinic carbon or from carbonyl carbons in HCO_3^- groups. Some results for various bicarbonate structures have shown that the typical chemical shift value of the carbonyl carbons in HCO_3^- groups is about 162 ppm.¹⁶ Thus, the line at 162.2 ppm (4) can be attributed to this group, while the line at 161.3 ppm is assigned to the guanidine carbon (3). The broader line width observed for the 161.3 ppm line is further evidence that it can be attributed to the guanidine carbon. It is well known that spin $1/2$ nuclei in a non-symmetric environment attached to quadrupole moments (such as ^{14}N) present a strong non-homogeneous line broadening in the solid state, which is consistent with the spectrum observed in Figure 1c. These results should be understood bearing in mind that the ionic bicarbonate structure **Ib** does not dissolve in CDCl_3 , while the carbamate **Ic** and zwitterionic carbamate **Ia** dissolves and, because they are not stable in the apolar media, CO_2 is released.

Comparing the experimental spectrum with the calculated values in Table 1, we see that the calculations predict different relative positions between the HCO_3^- carbon and the guanidine carbon (3). The experimental shift for the guanidine carbon is, however, consistent with the calculated value for protonated TMG. This would suggest that the TMGH- HCO_3^- geometry utilized in the calculations is not representative of the geometry of the complex in experiment.

Although the solution spectra were quite elucidating in terms of understanding the products formation, the main interest in this work is to characterize them as they were obtained, i.e., in the solid phase. The ^{13}C CP/MAS spectrum of the TMG- CO_2 solid product is shown in Figure 2a. In order to avoid chemical decomposition after the preparation, the product was kept at -30°C , which is also the measuring temperature. As it can be observed, the spectrum is composed of six distinguishable lines, with chemical shift values of 39.5 (1,2), 41.2 (5), 43.1 (6), 153.1 (8), 159.1 (7), 161.7 (3), and 162.3 (4) ppm. Taking into consideration the evidence that two structures were formed, see Scheme 1, one can evaluate the consistency of the spectrum based on such structures. The NMR lines within the 39–44 ppm region have typical chemical shift values of methyl

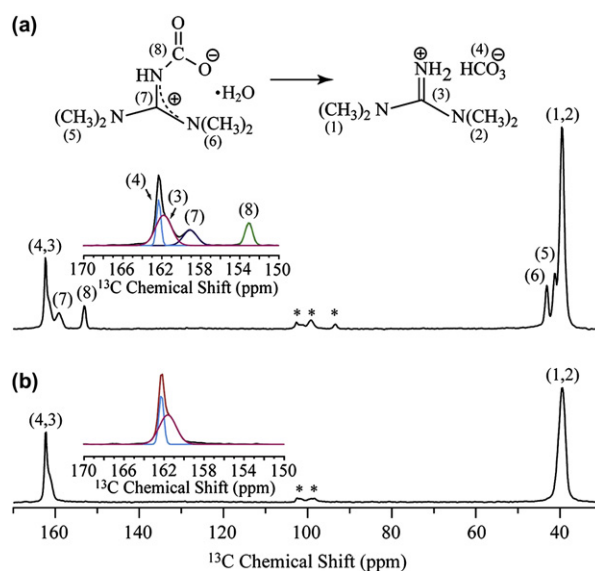


Figure 2. ^{13}C CP/MAS spectra of TMG- CO_2 at -30°C . (a) Spectrum of the reaction mixture at the end of the reaction (**Ia** and **Ib** in Scheme 1). The inset shows a zoom of the 150–170 ppm region. (b) Spectrum after 30 min of drying under reduced pressure. The inset shows a zoom of the 150–170 ppm region. Spinning side bands are indicated by asterisk (*) in the spectra.

be either from guanidinic carbon or from carbonyl carbons in the HCO_3^- groups. From the proposed chemical structures shown in Scheme 1 several non-NMR equivalent NCH_3 should be expected (the methyl groups may be non-equivalent due to restricted conformational rotation on the NMR time scale, with one pair of methyl groups being closer to the NCOO^- group than the other). Since the main effect of the positive charge is to change the CH_3 carbons to higher parts per million values, it is possible to attribute it to the CH_3 lines as indicated in Figure 2a. The assignment of these groups as methyl groups was confirmed by measuring the local residual CH dipolar coupling using 1D-DIPSHIFT experiments (not shown).¹⁷ The measured values were 7.3 kHz for the three carbons, which is typical of CH_3 end groups that execute a fast rotation around the local C_3 axis. Based on the previous discussion, the line at 162.3 ppm can be attributed to the HCO_3^- carbon in structure **1b**. The assignment of the remaining lines can be made considering that chemical shift for non-charged guanidine structures, the guanidinic carbon, was observed at about 157–160 ppm.¹⁸ Because of the proposed structure with which the carbons are positively charged, the lines at 159.1 and 161.7 ppm should be consistent with the guanidinic carbons in the structures **1a** and **1b**, respectively. Finally, the line at 153.1 ppm is attributed to the carbonyl carbons bonded to ^{14}N in structure **1a**. With these assumptions, a possible assignment to the ^{13}C CP/MAS spectrum is shown in Figure 2a. The ^{13}C CP/MAS NMR spectra are consistent with the simultaneous presence of carbamate and bicarbonate solid-state products.

Comparison between experimental and the quantum mechanical chemical shifts (Table 1) do in general support the conclusions drawn on speciation. The main uncertainty is perhaps if a zwitterionic carbamate (**1a**) or carbamate (**1c**) is formed. The calculated shifts for **1c** are closer to the experimental values, given the

uncertainty in calculations it is hard to draw any confident conclusions on this point.

An interesting behavior was also observed when the sample was dried under reduced pressure for 30 min. The ^{13}C CP/MAS spectrum, after this treatment, is shown in Figure 2b. As can be observed, lines attributed to carbons numbered as 5, 6, 7, and 8 disappeared from the spectrum, leaving the lines from carbons numbered as 1, 2, 3, and 4. Figure 2b also shows that after drying the sample the line width of the signal corresponding to the methyl groups is larger than before, which indicates that this signal can be attributed to methyl groups with slightly different chemical shifts. It can be also observed that the spectrum shown in Figure 2b is almost identical to that in Figure 1b, which shows that the final product obtained either by dissolving the TMG-CO_2 in CDCl_3 or by vacuum drying are indeed the same. This confirms the formation of a highly stable ionic bicarbonate structure **1b** and a species (**1a** or **1c**) that releases CO_2 under a proper treatment.

^{13}C and ^1H NMR of TBD-CO_2 . Solution ^1H and ^{13}C NMR spectra were acquired in order to identify the reaction products from fixation of CO_2 by TBD guanidine. In this case, because the expected structures are more complex than in the case of TMG-CO_2 , HSQC and HBMBC experiments¹⁹ were also carried out. Figure 3a shows the ^{13}C solution NMR spectrum of the TBD and CO_2 reaction product. The lines at 115.92 ppm and within the 75.72–78.47 ppm region are due to the presence of CDCl_3 and residual acetonitrile (ACN) in the solution and will be disregarded. The presence of only three non-equivalent CH_2 carbons at 20.00, 37.98, and 45.95 ppm is not consistent with a fixed $\text{C}=\text{N}^+$ bond as shown in structures **11a–11c** (Scheme 2), but it suggests that the CDCl_3 soluble part of the product assumes a resonant structure as shown in the inset of Figure 3a. Hence, the basic structure shown in the inset of Figure 3a

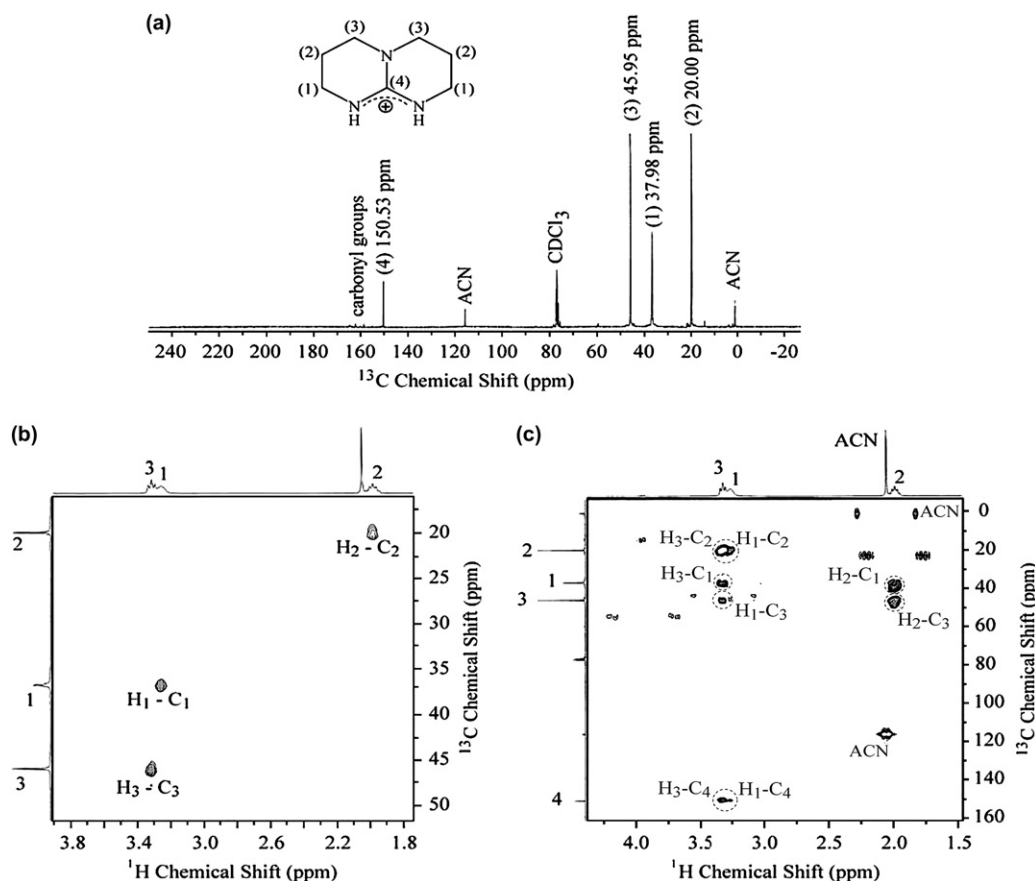


Figure 3. (a) ^{13}C 1D solution, (b) HSQC, and (c) HMBBC spectra of TBD-CO_2 reaction product.

will be used for the interpretation of the 2D HSQC and HMBC spectra. Figure 3b shows the region of the HSQC spectra where the cross-peaks indicate the ^1H nuclei directly attached to ^{13}C . Thus, from the spectrum shown in Figure 3b the following set of CH_2 pairs can be assigned: ^{13}C at 21.00 ppm and ^1H at 1.95 ppm (C3–H3); ^{13}C at 38.00 ppm and ^1H at 3.25 ppm (C2–H2); ^{13}C at 45.95 ppm and ^1H at 3.33 ppm (C1–H1). Further assignments can be obtained from the HMBC spectrum shown in Figure 3c. The long-range HMBC spectrum is shown through bond correlation between ^1H and ^{13}C nuclei. As can be observed, there are no long-range correlations between the ^1H line at 1.95 ppm and the ^{13}C line at 150.53 ppm (attributed to the chemical shift value of carbamic carbon C4). Thus, this ^1H nucleus must be four bonds away from C4, which means that this line can be attributed to H in the position 2 of Figure 3a. Therefore, the pair ^{13}C at 38.00 ppm and ^1H at 3.25 ppm can be assigned to the C2–H2 group. Both ^1H lines at 3.25 and 3.33 ppm show three bond correlations with C4, but the correlation is clearly weaker for the line at 3.33 ppm, which suggests that it occurs through the resonant double bond. In addition, the broadening of this line also suggests a higher proximity to a positive charge. Hence, the line at 3.33 ppm is attributed to the ^1H nuclei in the position 1 of Figure 3a and, consequently, the pair ^{13}C at 38.00 ppm and ^1H at 3.25 ppm is assigned to the C1–H1 group. These assignments are in agreement with the two bond correlations shown in the HMBC spectrum. Consequently, these results are consistent with the formation of a structure that contains the basic unit shown in Figure 3a, and the presence of extra peaks in the 150–170 ppm region of the ^{13}C NMR spectrum suggests that all three structures could be formed.

The solution NMR analysis of the TBD and CO_2 reaction products was quite elucidating in terms of obtaining the initial line assignments. However, the reaction products are solid powders and it is important to characterize them in the solid phase. The ^{13}C CP/MAS spectrum of the TBD– CO_2 product at -30°C is shown in Figure 4. As with TMG– CO_2 , it is possible to observe the presence of NMR lines from 150 to 170 ppm and from 20 to 50 ppm. However, in this case, there are at least six lines at 150 ppm region (165.4, 162.3, 157.0, 155.0, 154.3, and 151.5 ppm) and several lines from 20 to 50 ppm, which can be divided in three groups with chemical shifts within the 42–50, 30–42, and 15–30 ppm regions. This is in agreement with the ^{13}C solution spectrum, making it possible to attribute them to the CH_2 ring carbons. However, in the solid state, each of these lines is composed by several lines, which can be due either to the fact that the lines on the right side, numbered 1, 2, and 3, and on the left side, 1', 2', and 3', are no longer NMR equivalents in the solid

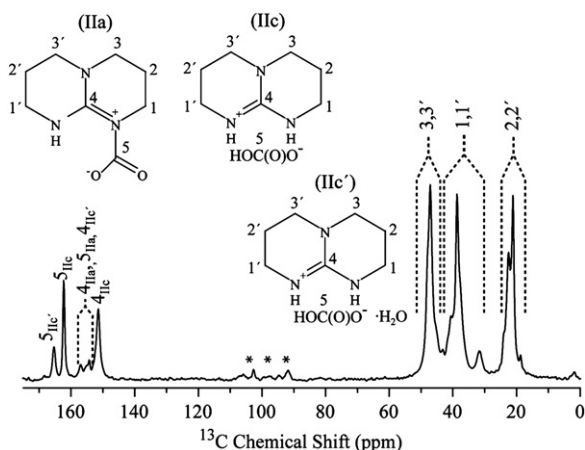


Figure 4. ^{13}C CP/MAS spectrum of TBD– CO_2 at -30°C . The NMR lines were attributed on the basis of the typical chemical shifts values assigned in the solution spectrum. Spinning side bands are indicated by asterisk (*) in the spectrum.

state or due to the presence of near structurally related compounds (from Scheme 1) as shown in the inset of Figure 4. More specific information about the formation of different compounds can be obtained from the 150 to 170 ppm region. As in the case of the TMG– CO_2 reaction product, the line at 162.3 ppm can be attributed to the carbon nucleus of HCO_3^- groups in a bicarbonate structure,^{16a} as represented by structure IIc in Scheme 2 (carbon 5_{IIc}). The four lines at 151.5, 155.0, 154.3, and 157 ppm are in a chemical shift region (150–160 ppm) that could be assigned either to guanidinic carbons or carbamic carbonyls.¹⁸ Since the intensity of the 151.5 and 162.3 ppm lines is comparable, the line at 151.5 ppm can most likely be attributed to the guanidinic carbon in a bicarbonate structure, such as IIc (carbon 4_{IIc}). Besides, given the possibility of the formation of a carbamate structure such as IIa, and the chemical shift calculation shown in Table 1, one can suggest that the 157.0 and 155.0 ppm lines are attributable to a guanidinic carbon and a carbamic carbonyl. Note that these two lines have similar intensities, which are in agreement with the above suggestion. Concerning the line at 165.4 ppm (5'_{IIc}), it appears in a chemical shift region that is neither typical of a guanidinic carbon nor typical of a carbamic carbonyl. However, it would be consistent with a bicarbonate carbonyl with a slightly different chemical environment from the one responsible for the 162.3 ppm line. This is consistent with the presence of water as suggested in the literature,^{16a} where a deshielding of the carbonyl carbon (shift to higher frequencies) is expected. Note also that in the presence of solvated bicarbonate, the guanidinic carbon signal is expected to be a little up-field, which is consistent with the line at 154.3 ppm (note also that the line intensity is consistent). Thus, the CPMAS spectrum is consistent with the formation of a carbamate structure (<20%) and a bicarbonate structure (>80%), as shown in the assignments of Figure 4. However, it should be pointed out that the assignment was made considering the formation of only these structures; the formation of structures with similar chemical composition cannot be ruled out. In fact, assigning peaks in these solid-state systems is not a trivial task. As a result of the inherent broadening of the ^1H signal due to the H–H dipolar interaction, the C–H correlation experiments are of less use in differentiating similar structures. Another approach would be C–N correlation spectra. Due to the strong quadrupolar interaction of the abundant ^{14}N nuclei, ^{15}N enrichment would be required in such experiments. Another issue is the non-quantitative character of the CPMAS experiments, which could compromise the analysis made in terms of the line intensities. However, since for analyzed non-protonated carbons the ^1H – ^{13}C CP transfer between non-bonded C–H pairs, which are at similar distances in all possible structures, it is expected to be similar. This allows the association of the line intensity with the relative amount of carbons of a given chemical species and validated the above analysis. In addition, in our experiments a radiofrequency ramp was used, which also makes the line intensities in the CPMAS more quantitative.¹⁸

The quantum mechanical chemical shifts are in general in good agreement with the interpretation given of the experimental spectrum. In Supplementary data, we provide an ^1H – ^{13}C plot from calculations showing good overall agreement with Figure 3b. The calculations suggest that carbon 4 on IIa and IIc and the carbamate carbonyl in IIa are likely to be the ones corresponding to the experimental lines in the 151–157 ppm range. Moreover, carbon 5 in bicarbonate (water solvated IIc' and non-solvated IIc) is expected to appear in the 162–170 ppm range. In fact, these features were considered in the attribution of the experimental spectrum of Figure 4. Calculations on the stability of IIb (Supplementary data) suggest that this species is perhaps too unstable to show up in the experimental spectrum. The five lines at 150 ppm may be all attributable to II, IIa and IIc, but there could also be some complex formed that we have not considered (perhaps a different form of bicarbonate complex).

Characterization of TMG–CO₂ and TBD–CO₂ by FTIR. The characterization by FTIR analyses of the products from the fixation of CO₂ with the bases TMG and TBD was limited to identify the bands that would indicate the presence of carbamate and/or carbonate groups. Hence, for TMG–CO₂ the spectrum showed two bands at ~1640 and ~1670 cm⁻¹ that can be attributed to bicarbonate and carbamate carbonyl groups, respectively. However, bands at ~1600 to 1700 cm⁻¹ could be associated to the presence of differently stabilized bicarbonates or carbonates compounds, e.g., guanidinium bicarbonate.^{12b,e} For the TBD–CO₂ products the FTIR spectrum showed a band at ~1717 cm⁻¹, which can be attributed to the carbamate carbonyl group. Nevertheless, the characteristic bands of bicarbonate can be superposed with the guanidine bands at ~1440 to 1650 cm⁻¹.

3.2. TGA–FTIR study of the CO₂ fixation with TMG and TBD guanidines

TGA–FTIR of the product TMG–CO₂. An interesting result was obtained when the product or a mixture of products TMG–CO₂ was analyzed by TGA. Figure 5 shows losses of CO₂ in both temperature ranges 15–38 and 38–74 °C.

These mass losses can be associated to the bands with higher values of absorbance at 27 and 59 °C attributed to free CO₂ (~2300 to 2400 cm⁻¹). In the spectrum shown in Figure 6, it can be observed more intense signals of CO₂ at 27 °C and less intense at 38 °C.

From the results of the TGA–FTIR study it can be proposed that there are at least two CO₂ containing compounds where the CO₂ molecule is bonded to guanidine TMG by two different bond types. One of these products presents a covalent bond N–CO₂ to form a carbamate and the other could be the ionic bicarbonate. This provides further support to the proposed TMG–CO₂ products **1a** and **1b** (shown in Scheme 1, Fig. 7).

The bicarbonate represented by **1b** should release CO₂ at higher temperature than the carbamic form **1a**. Thus, observing the TGA–FTIR in Figure 5 it is also reasonable to suppose that tetramethylguanidinium bicarbonate **1b** was formed in a relatively higher amount than carbamate **1a** by comparing the relative intensities of the CO₂ at different temperatures.

Fixation of CO₂ with guanidine TMG occurred by the formation of two products characterized as carbamate **1a** and bicarbonate **1b**. The CO₂ release from the TMG–CO₂ compounds has been observed

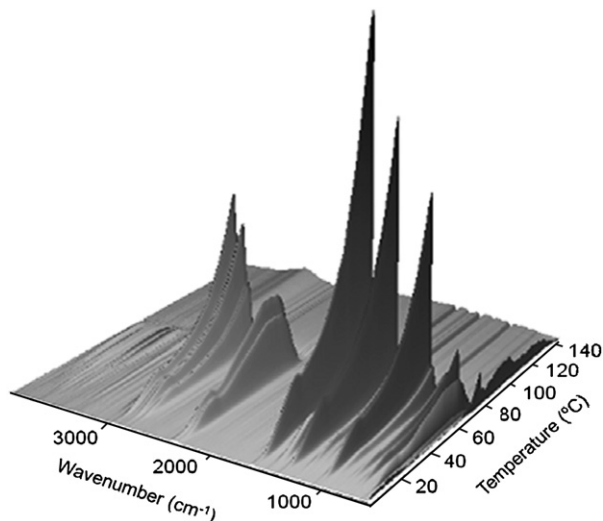


Figure 5. TGA–FTIR 3D-Diagram for TMG–CO₂.

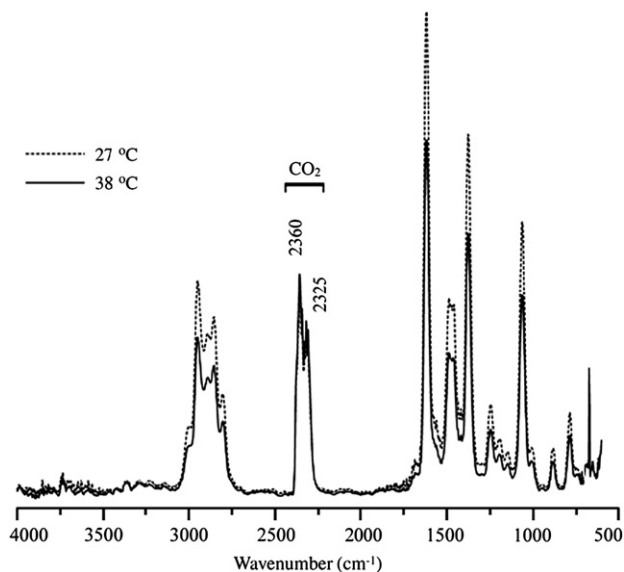


Figure 6. FTIR spectrum of the products from the thermal decomposition of TMG–CO₂.

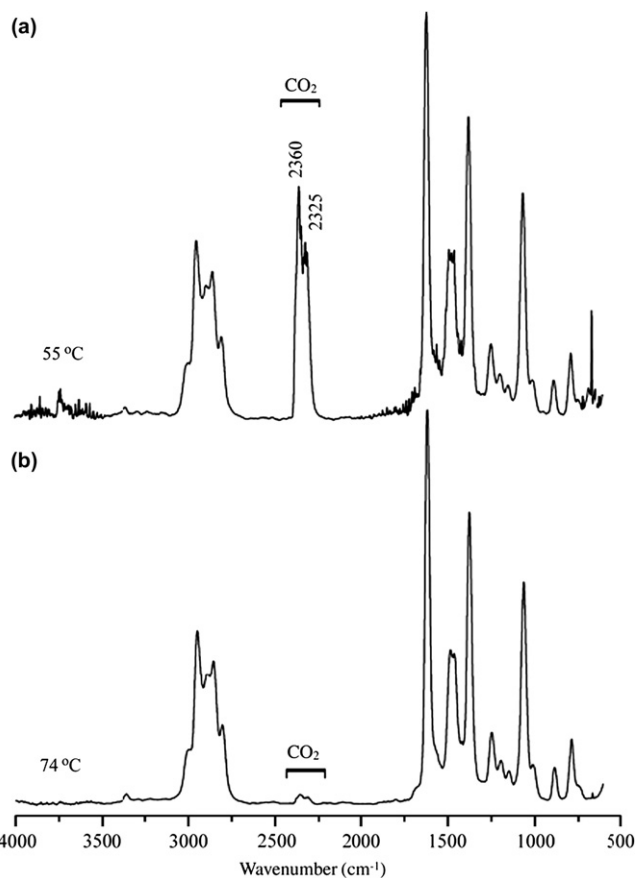


Figure 7. (a) FTIR spectra showing the bands attributed to CO₂ at ~2320 to 2360 cm⁻¹ (55 °C). (b) Material recovered only from TMG thermal decomposition indicating that at this temperature all CO₂ was released (74 °C).

not to be a significant process and it seems that compounds can be sublimated at moderated temperature at atmospheric pressure instead of a CO₂–TMG rupture. Thus, fixation and release of the CO₂ with TMG could be more important for transcarboxylation (kinetic reversible fixation) reactions and biological studies.

TGA–FTIR of TBD–CO₂. Figure 8 has shown at least three CO₂ losses at temperatures between 80 and 140 °C. These CO₂ losses can

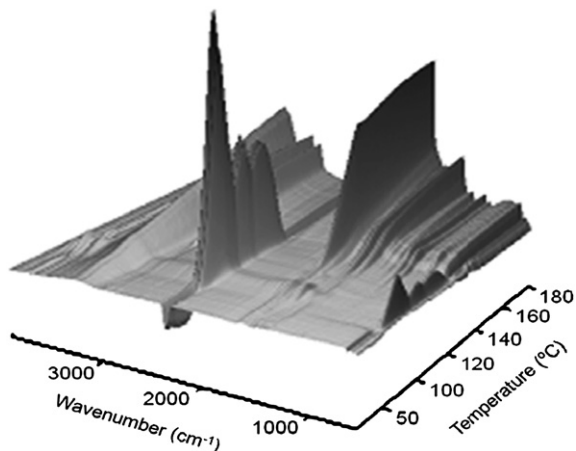


Figure 8. TGA-FTIR 3D diagram for TBD-CO₂.

be associated with the presence of three compounds and the CO₂ molecule could be bound in different ways to TBD moiety.

Figure 9 shows the FTIR bands corresponding to free CO₂ at 80 and 110 °C. These bands were also observed with less intensity at

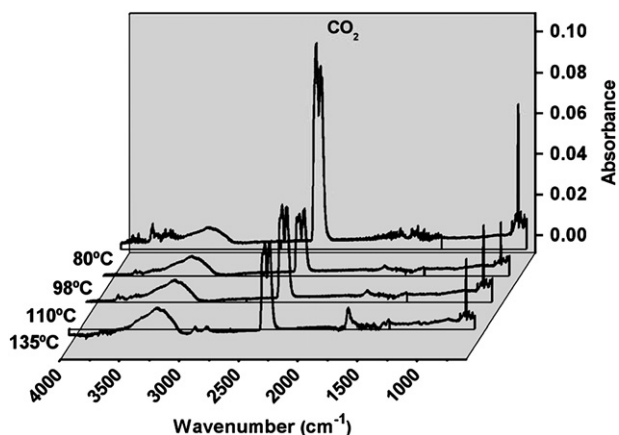


Figure 9. TGA-FTIR spectra of TBD-CO₂ versus temperature.

98 and 139 °C. The explanation for this behavior could be the presence of at least three products formed from the fixation of CO₂ with the guanidine TBD.

From the TGA-FTIR analyses of the products of the CO₂ fixation with guanidine TBD, it is possible to observe that at least three CO₂ losses were identified by typical bands of free CO₂ that have appeared with different intensities at temperatures between 80 and 140 °C.

This is in agreement with the NMR data that suggested the presence of three CO₂ containing products, with their structures as represented in Scheme 2. An interesting CO₂ releasing process from the TBD-CO₂ products was observed. On the other hand, TBD has a higher melting point (130–132 °C) than liquid TMG and compounds from the fixation of CO₂ with TBD can release CO₂ as the almost unique product from ~80 to 135 °C. Hence, TBD could be more useful for CO₂ selective fixation and releasing from a gas mixture. Therefore, TBD could be a promising model compound for industrial CO₂ separation.

3.3. Time-dependent isothermal absorption of CO₂ by TMG and TBD guanidines

The CO₂ fixation with the guanidines TMG and TBD was conducted in a TG instrument under a CO₂ flow (15 mL/min). The guanidines were placed on a sample pan in the TG instrument at three different temperatures and the experiments were carried out in an isothermal mode for a determined period of time or until the weight variation stopped.

Figure 10 shows the CO₂ absorption behavior of TMG at 22, 26, and 30 °C. The CO₂-fixation efficiency at 30 °C is lower than that at 26 °C. This could be related to the minor thermal stability of the TMG-CO₂ products as showed in Figure 6. A lower temperature resulted in higher amounts of CO₂ fixation owing to the entropic advantage.

The CO₂ absorption by TBD was also investigated at three different temperatures, at 30, 60, and 90 °C as showed in Figure 11. Mass losses of TBD at the beginning could be associated with some volatile solvent impurity (commercial TBD purity is around 98%). Hence, at 90 °C no mass loss was observed at the starting absorption experiment. At 90 °C the CO₂ absorption by TBD is in accordance with this temperature value being between 80 and 98 °C where CO₂ mass losses were observed from TBD-CO₂

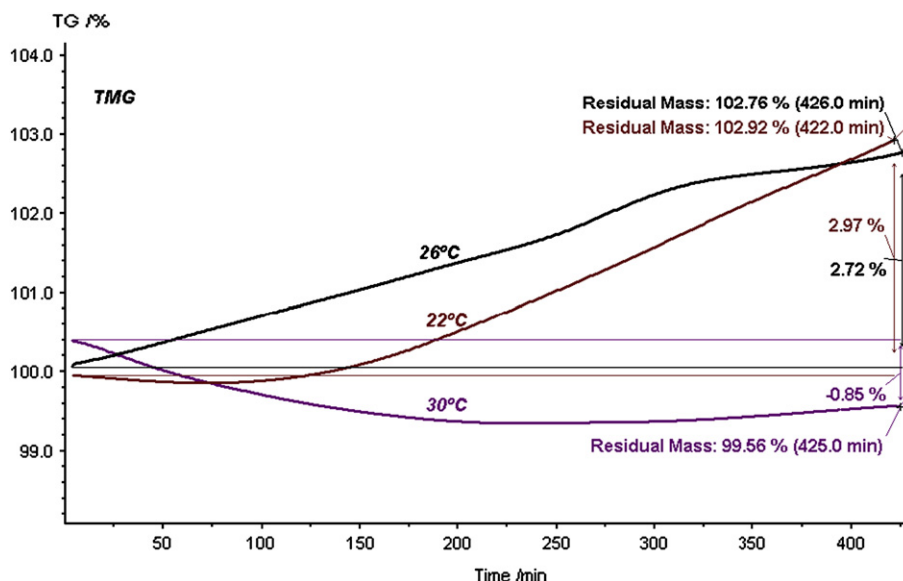


Figure 10. Isothermal CO₂ absorption by TMG.

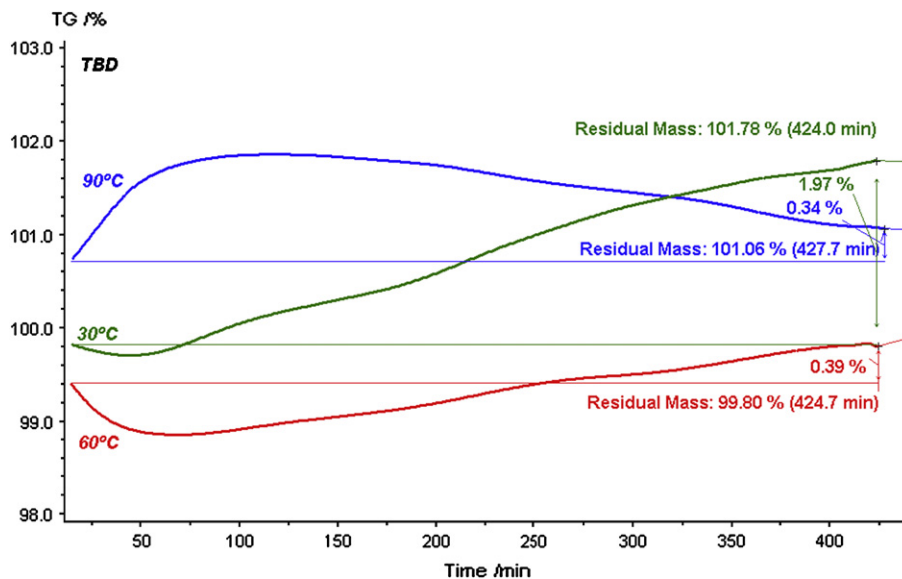


Figure 11. Isothermal CO₂ absorption by TBD.

products as displayed in Figure 9. On the other hand, after 150 min the mass absorption starts to decrease, which indicates a possible TBD–CO₂ product degradation or that no more CO₂ absorption is achieved at this time.

The guanidines were reacted with CO₂ and mass increases were observed. The mass increases at lower temperatures were larger than with higher temperatures, probably due to the better CO₂-fixation ability of guanidines at lower temperatures.

These results demonstrate the potential of the guanidines as recyclable CO₂ adsorption materials, which can fix CO₂ reversibly and release it at higher temperatures.

3.4. Transcarboxylation experiments

Kinetic reversibility. For the purpose of comparison, the transcarboxylation of cyclohexylamine, as a model nucleophilic amine, was performed at –5 °C with both TMG–CO₂ and TBD–CO₂, and the corresponding ethyl carbamates were obtained by a subsequent reaction of the carbamate intermediates with ethyl iodide for 6 h at 10 °C. At low temperatures alkylation of the amine or carbamate is minimal. General pathway for formation of carbamates from transference of CO₂ is illustrated in Scheme 3.

Under these conditions, the yields of the isolated *N*-(cyclohexyl) ethyl carbamate were 77 and 68%, respectively. Another ethyl and butyl carbamates were also prepared by transcarboxylation of furfuryl- and 2,4-dichlorobenzylamine. Structures were confirmed by NMR analyses and GC conversion to carbamates was ~70 to 80% (no optimized reactions). Table 2 summarizes the approximated yields of isolated alkyl carbamates from each guanidine–CO₂ products.

From these results, we can say that CO₂ fixation with both guanidines, TMG and TBD, is a kinetically reversible process as the corresponding fixation products have shown to be useful as

Table 2

Results from transcarboxylation of amines with Guanidine–CO₂ products

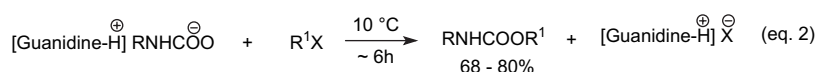
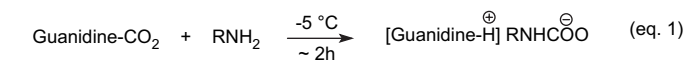
Carbamate	R	R ₁ X	Yield of carbamates obtained by transcarboxylation	
			TMG–CO ₂ (%)	TBD–CO ₂ (%)
3	C ₆ H ₁₁	Etl	77	68
4	C ₅ H ₅ O	Etl	80	72
5	C ₇ H ₅ Cl ₂	Etl	74	69
6	C ₅ H ₅ O	BuBr	76	70
7	C ₇ H ₅ Cl ₂	BuBr	78	70

transcarboxylating compounds. Selective transcarboxylation from carbamate or bicarbonate intermediates is under current investigation and the results will be opportunely communicated.

This method for preparation of carbamates is limited to transcarboxylation of compound with higher nucleophilicity than the initial CO₂ trap (TMG and TBD), because reaction of the corresponding TMG and TBD carbon dioxide complexes did not transfer the CO₂ moiety toward alcohols.

4. Conclusions

Guanidines TMG and TBD can be used as model compounds by capture and activation of the CO₂ molecule. These bases form bicarbonates presumably by previous formation of water-solvated carbamic intermediate. The guanidine–CO₂ products can transcarboxylate nucleophilic amines. This behavior suggests a mimetic transcarboxylase activity. On the other hand, bicarbonate formation in the presence of the investigated guanidines, CO₂, and catalytic water is indicative of the non-metal carbonic anhydrase mimetism. This is very interesting for biochemical study of the guanidine related compound, which can be used for CO₂ and water fixation. Finally, TBD–CO₂ products have shown an interesting thermal



Scheme 3.

stability. Releasing of CO₂ from the TBD–CO₂ products has occurred at moderated temperature. This could be useful for selective separation of CO₂ from complex gas mixtures by TBD or TBD related compounds.

5. Experimental section

5.1. Fixation of CO₂ with 1,1,3,3-tetramethylguanidine (TMG) and 1,3,4,6,7,8-hexahydro-2H-pyrimido[1,2-a]-pyrimidine (TBD), compounds I and II, respectively: general procedure

The CO₂-fixation experiments with the guanidine bases have been carried out using pure commercially available TMG (99%, GC) and TBD (98%) without any previous purification. Reactions were carried out in the presence or absence of organic solvent (fresh acetonitrile) for liquid TMG or using minimal acetonitrile for TBD. Experiments using melted TBD were not successful for CO₂ capture, presumably because of low CO₂ retention into the reaction media. No significant differences were observed under solvent or dry conditions for TMG. Guanidines (5 mmol) were placed in a 50-mL two-neck round flask and acetonitrile was added if needed, then CO₂ was bubbled under normal pressure (~10 mL/min) at 5 °C with magnetic stirring for 2 h. A high yield of a white powder (~90%) was obtained for both TMG and TBD–CO₂-captured products. These crude products were stored at 0 °C for liquid-state NMR (¹H and ¹³C), solid-state NMR, ¹³C, FTIR, and TGA–FTIR measurements. It should be noted that while the intention has been to carry out experiments in a water-free environment both TMG and TBD are highly hygroscopic species and water contamination cannot be ruled out. Even small quantities of water may have a significant effect on the overall reactivity of the systems. On the other hand, experiments carried out under no especially anhydrous condition can be interesting for future applications.

5.2. NMR studies of the TMG–CO₂ and TBD–CO₂ products

Solid-state NMR experiments were performed at ¹³C and ¹H frequencies of 100.5 and 400.0 MHz, respectively. A VARIAN 7-mm MAS double-resonance probe head with variable temperature (VT) was used. Typical $\pi/2$ pulse lengths of 3.5 and 4.0 ms were applied for ¹³C and ¹H, respectively. Time Proportional Phase Modulated (TPPM) ¹H decoupling with field strength of 70 kHz, cross-polarization with radiofrequency ramp²⁰ with duration of 1 ms, MAS spinning frequency of 6 kHz, and recycle delays of 5 s were used.

Liquid-state NMR experiments were performed at ¹³C and ¹H frequencies of 75 and 300.0 MHz, respectively. Typical $\pi/2$ pulse lengths of 7 and 10 μ s were applied for ¹³C and ¹H, respectively. Recycle delays of 0.1 and 1 s and 16 and 64 K acquisition points were used. The 2D experiments were carried out using 4 K points in the direct dimension and 256 t_1/ω_1 increments in the indirect dimension.

TGA–FTIR study for TMG–CO₂ and TBD–CO₂. The study was carried out with a coupled TG–FTIR, in which all gas evaporated at the TG chamber is channeled to the FTIR spectrometer. The samples (5.0 mg) were heated in alumina crucible using purified N₂ gas (15 mL/min) and heating rate of 10 °C/min from 0 °C to 140 °C. FTIR spectra were recorded in the wavenumber range 400–4000 cm⁻¹ with 4 cm⁻¹ spectral resolution, 32 scans, and a DTGS detector.

5.2.1. 1,1,3,3-Tetramethylguanidine (I)

¹H NMR (CDCl₃) δ 2.65 (s, 12H, 4CH₃), 4.94 (s, 1H, NH); ¹³C (CDCl₃) δ 39.19 (CH₃), 167.8 (C=N), all spectra were carried out at room temperature.

5.2.2. 1,1,3,3-Tetramethylguanidine-N-carboxylate (Ia)

Assigned by solid-state ¹³C{¹H} NMR δ 41.2 (CH₃), 43.5 (CH₃), 159.1 (C=N), 153.8 (–NCOO); IR 1640, 1670 cm⁻¹, these bands can

be attributed to bicarbonate and carbamate carbonyl groups, respectively.

5.2.3. 1,1,3,3-Tetramethylguanidinium bicarbonate (Ib)

Assigned based on the ¹H liquid state by ¹H NMR peaks of the soluble TMG compound (as described above) and in the solid-state ¹³C CPMAS NMR δ 41.2 (CH₃), 161.7 (C=N), 162.3 (HCO₃⁻). IR bands at ~1600 to 1700 cm⁻¹ could be associated to the presence of differently stabilized bicarbonates or carbonate compounds, e.g., guanidinium bicarbonate.^{12b,e}

5.2.4. 1,3,4,6,7,8,9-Hexahydro-2H-pyrimido[1,2-a]-pyrimidin-1-ium-1-carboxylate (IIa)

Assigned based on the ¹³C solid-state NMR δ 165.4 (–COO⁻), 157.5 (–N=C=N⁺). IR ~1717 cm⁻¹, which can be attributed to the carbamic C=O group.

5.2.5. 1,3,4,6,7,8-Hexahydro-2H-pyrimido[1,2-a]-pyrimidinium bicarbonate (IIc)

Assigned based on the ¹³C solid-state NMR δ 162.3 (HOCO⁻), 152 (–N=C=N⁺) indicates that compound IIc was also formed. The lines at the 20–50 ppm region are consistent either with IIa or IIc. Compound IIc was also identified by liquid-state NMR using ¹H, ¹³C{¹H}, HSQC, and HMBC correlation spectroscopy and the assignment of these signals was ¹³C at 21.00 ppm and ¹H at 1.95 ppm (C3–H3); ¹³C at 38.00 ppm and ¹H at 3.25 ppm (C2–H2); ¹³C at 45.95 ppm and ¹H at 3.33 ppm (C1–H1). IR ~1440 to 1650 cm⁻¹, in this region characteristic band of bicarbonate can be superposed with the guanidine bands.

5.3. Transcarboxylation experiments for N-alkyl carbamates by amine transcarboxylation

In a typical procedure, 2 mmol of amine was slowly added to the suspension of guanidine–CO₂ (2.4 mmol) in 10 mL of anhydrous acetonitrile, with stirring for 1.5 h at 5 °C. Then, alkyl halide (3 mmol) was poured into the solution and the reaction mixture was stirred at ambient temperature for an additional 6 h. Evaporation of the solvent and extraction with ethyl ether (3×10 mL) or alternative column chromatography (6:1 hexanes/EtOAc) gave the corresponding N-alkyl carbamates.

5.3.1. N-(Cyclohexyl) ethyl carbamate (3)

White solid; mp 122–124 °C (from ether); ¹H NMR (200.13 MHz, CDCl₃) δ 1.27–1.09 (m, 9H, CH₂ cyclohexyl+CH₃), 1.60 (m, 2H, CH₂ cyclohexyl), 1.91 (m, 2H, CH₂ cyclohexyl), 3.41 (m, 1H, CH cyclohexyl), 4.07 (q, 2H, CH₂), 4.53 (s, 1H, NH); ¹³C NMR (50.32 MHz, CDCl₃) δ 14.5, 24.7, 25.4, 33.4, 49.6, 66.0, 155.8 (C=O); MS (70 eV) m/z 56 (100%), 128, 142, 171 (M⁺). IR (KBr) 3340, 3223, 1680 cm⁻¹.

5.3.2. N-(2-Furfuryl) ethyl carbamate (4)

Yellow oil; ¹H NMR (200.13 MHz, CDCl₃) δ 1.24 (t, 3H, methyl), 4.11 (q, 2H, CH₂), 4.29 (d, 2H, CH₂ furyl), 5.05 (t, 1H, amino), 6.20 (d, 1H, 3-furyl), 6.29 (2d, 1H, 4-furyl), 7.32 (d, 1H, 5-furyl). ¹³C NMR (50.32 MHz, CDCl₃) δ 15.3, 37.9, 61.0, 107.0, 109.5, 142.1, 151.6, 156.3 (C=O). MS (70 eV) m/z 69, 81, 96 (100%), 140, 169 (M⁺). IR (thin film) 3336, 1679, 1312 cm⁻¹.

5.3.3. N-(2-Furfuryl) butyl carbamate (5)

Yellow oil; ¹H NMR (200.13 MHz, CDCl₃) δ 0.94 (t, 3H, CH₃), 1.50 (m, 2H, CH₂), 1.62 (m, 2H, CH₂ furyl), 4.09 (t, 2H, CH₂), 5.01 (t, 1H, NH), 6.23 (d, 1H, 3-furyl), 6.31 (2d, 1H, 4-furyl), 7.34 (d, 1H, 5-furyl); ¹³C NMR (50.32 MHz, CDCl₃) δ 13.9, 20.1, 27.3, 36.0, 61.7, 107.2, 109.2, 151.4, 156.1 (C=O); MS (70 eV) m/z 57, 69, 81, 96 (100%), 136, 193 (M⁺). IR (thin film) 3332, 1677, 1311 cm⁻¹.

5.3.4. *N*-(2,4-Dichlorobenzyl) ethyl carbamate (6)

Yellow oil; ^1H NMR (250 MHz, DMSO- d_6) δ 1.20 (t, 3H, CH₃), 4.08 (q, 2H, CH₂), 4.62 (2d, 2H, CH₂ benzyl), 6.55 (t, 1H, NH), 7.00 (d, $J=8.4$ Hz, 1H, ArH), 7.19 (2d, $J=2.0, 8.4$ Hz, 1H, ArH), 7.40 (d, $J=2.2$ Hz, 1H, ArH). ^{13}C NMR (62.50 MHz, DMSO- d_6) δ 14.4, 44.7, 61.6, 127.0, 129.6, 133.2, 134.0, 136.4, 136.6, 157.6 (C=O); MS (EI, 70 eV) m/z 45, 87, 159, 161, 201 (100%), 203 (64%), 247 (M⁺), 249 (M⁺+2); IR (thin film) 3340, 1680 (C=O), 1582–1540 (Ar) cm⁻¹.

5.3.5. *N*-(2,4-Dichlorobenzyl) butyl carbamate (7)

Yellow oil; ^1H NMR (250 MHz, DMSO- d_6) δ 0.92 (t, 3H, CH₃), 1.55 (m, 2H, CH₂), 1.68 (m, 2H, CH₂), 4.10 (t, 2H, CH₂), 4.59 (2d, 2H, CH₂ benzyl), 6.58 (t, 1H, NH), 7.01 (d, $J=8.4$ Hz, 1H, ArH), 7.21 (2d, $J=2.0, 8.4$ Hz, 1H, ArH), 7.41 (d, $J=2.2$ Hz, 1H, ArH); ^{13}C NMR (62.50 MHz, DMSO- d_6) δ 13.6, 19.2, 31.9, 44.7, 64.6, 126.8, 129.5, 133.0, 133.8, 136.5, 137.0, 158.0 (C=O); MS (EI, 70 eV) m/z 57, 73 (100%), 159, 161, 201, 203, 275 (M⁺), 277 (M⁺+2); IR (thin film) 3343, 1681 (C=O), 1580–1540 (Ar) cm⁻¹.

Acknowledgements

Authors acknowledge Prof. José A. Giacometti (FCT–UNESP) for his fundamental support to this research on chemistry of carbon dioxide. They also acknowledge Dr. Paulo J.M. Cordeiro and Dr. Mauro R. Fernandes (IQSC–USP) for GC–MS and FTIR analyses, Prof. Cláudio F. Tormena (NMR Laboratory, IQ–UNICAMP) for providing the NMR spectrometer for the solution analyses. Finally, authors are grateful to the Brazilian Agencies FAPESP, CAPES, and CNPq.

Supplementary data

Quantum mechanical chemical shift data and reaction energies. Supplementary data associated with this article can be found in the online version, at doi:10.1016/j.tet.2008.08.008.

References and notes

1. *Climate Change 2007: The Physical Science Basis*; Solomon, S., Qin, D., Manning, M., Chen, Z., Marquis, M., Averyt, K. B., Tignor, M., Miller, H. L., Eds.; Contribution of Working Group I to the Fourth Assessment Report of the Intergovernmental Panel on Climate Change; Cambridge University Press: Cambridge, United Kingdom and New York, NY, USA, 2007.
2. *IPCC Special Report on Carbon Dioxide Capture and Storage Prepared by Working Group III of the Intergovernmental Panel on Climate Change*; Metz, B., Davidson, O., de Coninck, H. C., Loos, M., Meyer, L. A., Eds.; Cambridge University Press: Cambridge, United Kingdom and New York, NY, USA, 2005.
3. Mcghee, W.; Riley, D. *J. Org. Chem.* **1995**, *60*, 6205–6507.
4. (a) Casadei, M. A.; Inesi, A.; Moracci, F. M.; Rossi, I. *Chem. Commun.* **1996**, 2575; (b) Stastny, V.; Rudkeviich, D. *M. J. Am. Chem. Soc.* **2007**, *129*, 1018–1019.
5. (a) *The Merck Index*, 12th ed.; Whitehouse Station: New Jersey, NJ, 1996; (b) *Hazardous Chemicals Desk Reference*, 4th ed.; John Wiley & Sons: New York, NY, 1998.
6. Delseth, R. *Chimia* **1998**, *52*, 698–701.
7. (a) Pérez, E. R.; Odnicki da Silva, M.; Costa, V. C.; Rodrigues-Filho, U. P.; Franco, D. W. *Tetrahedron Lett.* **2002**, *43*, 4091–4093; (b) Pérez, E. R.; Santos, R. H. A.; Gambardella, M. T. P.; de Macedo, L. G. M.; Rodrigues-Filho, U. P.; Launay, J.-C.; Franco, D. W. *J. Org. Chem.* **2004**, *69*, 8005–8011.
8. Endo, T.; Nagai, D.; Monma, T.; Yamaguchi, H.; Ochiai, B. *Macromolecules* **2004**, *37*, 2007–2009.
9. Darensbourg, D. J.; Mackiewicz, R. M. *J. Am. Chem. Soc.* **2005**, *127*, 14026–14038.
10. Heldebrant, D. J.; Jessop, P. G.; Thomas, C. A.; Eckert, C. A.; Liotta, C. L. *J. Org. Chem.* **2005**, *70*, 5335–5338.
11. (a) Jessop, P. G.; Heldebrant, D. J.; Li, X.; Eckert, C. A.; Liotta, C. L. *Nature* **2005**, *436*, 1102; (b) Yamada, T.; Lukac, P. J.; George, M.; Weiss, R. G. *Chem. Mater.* **2007**, *19*, 967–969.
12. (a) Amatore, C.; Saveant, J.-M. *J. Am. Chem. Soc.* **1981**, *103*, 5021–5023; (b) Christensen, P. A.; Hamnett, A.; Muir, A. V. G. *J. Electroanal. Chem.* **1990**, *288*, 197–215; (c) Genaro, A.; Isse, A. A.; Severin, M. A.; Vianello, E.; Bhugun, I.; Saveant, J.-M. *J. Chem. Soc., Faraday Trans.* **1996**, *92*, 3963–3968; (d) Casadei, M. A.; Inesi, A.; Rossi, I. *Tetrahedron Lett.* **1997**, *38*, 3565–3568; (e) Perez, E. R.; Garcia, J. R.; Cardoso, D. R.; McGarvey, B. R.; Batista, E. A.; Rodrigues-Filho, U. P.; Vielstich, W.; Franco, D. W. *J. Electroanal. Chem.* **2005**, *578*, 87–94; (f) Feroci, M.; Orsini, M.; Rossi, I.; Sotgiu, G.; Inesi, A. *J. Org. Chem.* **2007**, *72*, 200–203.
13. Wiberg, K. B. *J. Comput. Chem.* **1999**, *20*, 1299–1333.
14. Cancas, M. T.; Mennucci, V.; Tomasi, J. *Chem. Phys.* **1997**, *107*, 3032–3041.
15. Frisch, M. J.; Trucks, G. W.; Schlegel, H. B.; Scuseria, G. E.; Robb, M. A.; Cheeseman, J. R.; Montgomery, J. A., Jr.; Vreven, T.; Kudin, K. N.; Burant, J. C.; Millam, J. M.; Iyengar, S. S.; Tomasi, J.; Barone, V.; Mennucci, B.; Cossi, M.; Scalmani, G.; Rega, N.; Petersson, G. A.; Nakatsuji, H.; Hada, M.; Ehara, M.; Toyota, K.; Fukuda, R.; Hasegawa, J.; Ishida, M.; Nakajima, T.; Honda, Y.; Kitao, O.; Nakai, H.; Klene, M.; Li, X.; Knox, J. E.; Hratchian, H. P.; Cross, J. B.; Bakken, V.; Adamo, C.; Jaramillo, J.; Gomperts, R.; Stratmann, R. E.; Yazyev, O.; Austin, A. J.; Cammi, R.; Pomelli, C.; Ochterski, J. W.; Ayala, P. Y.; Morokuma, K.; Voth, G. A.; Salvador, P.; Dannenberg, J. J.; Zakrzewski, V. G.; Dapprich, S.; Daniels, A. D.; Strain, M. C.; Farkas, O.; Malick, D. K.; Rabuck, A. D.; Raghavachari, K.; Foresman, J. B.; Ortiz, J. V.; Cui, Q.; Baboul, A. G.; Clifford, S.; Cioslowski, J.; Stefanov, B. B.; Liu, G.; Liashenko, A.; Piskorz, P.; Komaromi, I.; Martin, R. L.; Fox, D. J.; Keith, T.; Al-Laham, M. A.; Peng, C. Y.; Nanayakkara, A.; Challacombe, M.; Gill, P. M. W.; Johnson, B.; Chen, W.; Wong, M. W.; Gonzalez, C.; Pople, J. A. *Gaussian 03, Revision C.02*; Gaussian: Wallingford, CT, 2004.
16. (a) Park, J.-Y.; Yoon, S. J.; Lee, H. *Environ. Sci. Technol.* **2003**, *37*, 1670–1675; (b) Hajduk, P. J.; Meadows, R. P.; Fesik, S. W. *Q. Rev. Biophys.* **1999**, *32*, 211–240.
17. (a) Hester, R. K.; Ackerman, J. L.; Neff, B. L.; Waugh, J. S. *Phys. Rev. Lett.* **1976**, *36*, 1081–1083; (b) Munowitz, M. G.; Griffin, R. G.; Bodenhausen, G.; Huang, T. H. *J. Am. Chem. Soc.* **1981**, *103*, 2529–2533.
18. Huang, M.-J.; Lee, K. S. *Mol. Phys.* **2005**, *103*, 2229–2237.
19. (a) Bodenhausen, G.; Ruben, D. *J. Chem. Phys. Lett.* **1980**, *69*, 185–189; (b) Bax, A.; Davis, D. G. *J. Magn. Reson.* **1985**, *63*, 207–213; (c) Bax, A.; Griffey, R. H.; Hawkins, B. L. *J. Magn. Reson.* **1983**, *55*, 301–315.
20. Novotny, E. H.; Hayes, M. H. B.; DeAzevedo, E. R.; Bonagamba, T. J. *Naturwissenschaften* **2006**, *93*, 447–450.